Building 3D Layer-by-Layer Graphene−Gold Nanoparticle Hybrid Architecture with Tunable Interlayer Distance

Chenming Xue,[†] Min Gao,[†] Yuhua Xue,[‡] Lin Zhu,[‡] Liming Dai,[‡] Augustine Urbas,[§] and Quan Li*[,†]
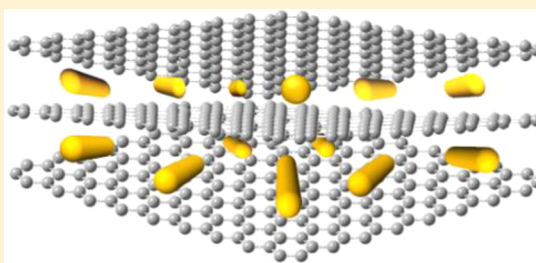
[†]Liquid Crystal Institute and Chemical Physics Interdisciplinary Program, Kent State University, Kent, Ohio 44242, United States
[‡]Department of Macromolecular Science and Engineering, Case Western Reserve University, Cleveland, Ohio 44106, United States
[§]Materials and Manufacturing Directorate, Air Force Research Laboratory, WPAFB, Dayton, Ohio 45433, United States

Ⓢ *Supporting Information*

ABSTRACT: The ability to construct self-assembled three-dimensional (3D) superstructures with desired functionality is not only of scientific curiosity but also crucial in the bottom-up nanofabrication of smart materials and devices. Here a facile solution-processable strategy for creating 3D layer-by-layer graphene−gold nanoparticle architectures was developed in which cysteine molecules with amino groups were chemically grafted onto the surface of graphene oxide and then the cysteine thiol groups were attached to the surface of gold nanorods (GNRs) through strong covalent Au−S linkages. In this self-assembled structure, as revealed by transmission electron microscopy (TEM) and scanning electron microscope (SEM), it was confirmed that the graphene layers aligned in parallel fashion rather than randomly to each other by the lying down patterns of the GNRs, which also formed layers in parallel. Furthermore, spherical gold nanoparticles with different sizes were used to control the interlayer distance of the 3D hybrid structure.

1. INTRODUCTION

Carbon nanomaterials, typically one-dimensional (1D) carbon nanotubes (CNTs) and two-dimensional (2D) graphenes, have captured great interest because of their uncommon thermal, electrical, and mechanical properties, which have potential for a wide range of applications such as energy generation and storage.[1−5] Currently, they are continually drawing more attention based on diverse architectures or systems, especially recent theoretical findings on 3D carbon architecture showing tremendous scientific potential.[6−9] Among carbon nanomaterials, graphene acting as a 2D nanosheet exhibits unique functionality.[10] However, one significant challenge for graphene is destacking from graphite because the planar polycyclic aromatic graphene sheets favor tight packing as a result of strong $\pi-\pi$ interactions, which limits the total accessible surface area critical for applications. With the assistance of gold nanoparticles (GNPs), graphene sheets can be destacked and stabilized, resulting in large surface area for various applications including supercapacitors.[11] On the other hand, because of the anisotropic graphene structure, it exhibits strong direction-dependent properties, including electrical transport, which is superior in the layer planes but extremely low across the planes. With such a 3D continual nanostructure, different layers of graphene can be connected by conducting GNPs. Thus, the poor interlayer electrical transport can be greatly enhanced. Moreover, applications based on the synergistic effect of GNPs/graphene hybrid materials could be developed.[12]

To build such a 3D nanostructure, here an easy solution-processable approach was developed by using graphene oxide (GO) as the starting material, because without functionalization the pristine graphene sheets are insoluble and very difficult to exfoliate, limiting their large-scale practical application.[1] For the synthesis, GO sheets are first chemically functionalized with the amino acid cysteine (Cys), which has an amine group to connect with GO, yielding GO-Cys, which was simultaneously significantly reduced. Because of the free thiol group of Cys, the resulting Cys-functionalized GO sheets are then linked with colloidal gold nanorods (GNRs) as the first tried sample through covalent Au−S linkages. When GNRs and graphene layers are continuously stacked on each other, a 3D layer-by-layer graphene−GNR hybrid nanostructure is created. Furthermore, spherical GNPs with different sizes can be used to build more such 3D structures, and the resulting layer-by-layer graphene−GNP nanostructures have tunable layer distances. These controlled 3D carbon nanostructures would not only help the understanding of structure−property relationships but also lead to various novel applications. For example, the assembled layer-by-layer reduced GO-GNP hybrid could be used for low-voltage flexible flash memory when forming a double-floating-gate structure.[13] For another aspect, exfoliated graphene separated by GNPs has the advantage of increased surface area for supercapacitor.[11]

2. EXPERIMENTAL SECTION

2.1. Materials and Instruments. All chemicals and solvents were purchased from commercial supplies and used

Report Documentation Page		Form Approved OMB No. 0704-0188

1. REPORT DATE **26 JUN 2014**	2. REPORT TYPE	3. DATES COVERED **00-00-2014 to 00-00-2014**

4. TITLE AND SUBTITLE	5a. CONTRACT NUMBER
Building 3D Layer-by-Layer Graphene-Gold Nanoparticle Hybrid Architecture with Tunable Interlayer Distance	5b. GRANT NUMBER
	5c. PROGRAM ELEMENT NUMBER
6. AUTHOR(S)	5d. PROJECT NUMBER
	5e. TASK NUMBER
	5f. WORK UNIT NUMBER
7. PERFORMING ORGANIZATION NAME(S) AND ADDRESS(ES) **Case Western Reserve University,Department of Macromolecular Science and Engineering,10900 Euclid Avenue,Cleveland,OH,44106**	8. PERFORMING ORGANIZATION REPORT NUMBER
9. SPONSORING/MONITORING AGENCY NAME(S) AND ADDRESS(ES)	10. SPONSOR/MONITOR'S ACRONYM(S)
	11. SPONSOR/MONITOR'S REPORT NUMBER(S)

12. DISTRIBUTION/AVAILABILITY STATEMENT
Approved for public release; distribution unlimited

13. SUPPLEMENTARY NOTES

14. ABSTRACT
The ability to construct self-assembled three-dimensional (3D) superstructures with desired functionality is not only of scientific curiosity but also crucial in the bottom-up nanofabrication of smart materials and devices. Here a facile solution-processable strategy for creating 3D layer-by-layer graphene???gold nanoparticle architectures was developed in which cysteine molecules with amino groups were chemically grafted onto the surface of graphene oxide and then the cysteine thiol groups were attached to the surface of gold nanorods (GNRs) through strong covalent Au???S linkages. In this self-assembled structure, as revealed by transmission electron microscopy (TEM) and scanning electron microscope (SEM), it was confirmed that the graphene layers aligned in parallel fashion rather than randomly to each other by the lying down patterns of the GNRs, which also formed layers in parallel. Furthermore, spherical gold nanoparticles with different sizes were used to control the interlayer distance of the 3D hybrid structure.

15. SUBJECT TERMS

16. SECURITY CLASSIFICATION OF:			17. LIMITATION OF ABSTRACT	18. NUMBER OF PAGES	19a. NAME OF RESPONSIBLE PERSON
a. REPORT **unclassified**	b. ABSTRACT **unclassified**	c. THIS PAGE **unclassified**	**Same as Report (SAR)**	**7**	

without further purification. HAuCl$_4$ is 30 wt % in diluted HCl solution. UV−visible spectra were collected on a PerkinElmer Lambda 25 UV−vis spectrometer at the resolution of 1 nm. For transmission electron microscopy (TEM) observation, solution samples were first dispersed on TEM Cu grids precoated with thin holey carbon film (Cu-400 HN) purchased from Pacific Grid Tech. After being completely dried, they were studied using a FEI Tecnai TF20 FEG TEM equipped with a 4k UltraScan charge-coupled device (CCD) camera for digital images. For the 3D tomography (TOMO) experiment, images were captured by tilting the sample between ±70 °C. For scanning electron microscopy (SEM), it is obtained in a FEI Quanta 450 FEG SEM. X-ray photoelectron spectroscopy (XPS) measurements were performed on a PHI 5000 VersaProbe spectrometer with an Al Kα X-ray source. The oxidation reduction reaction (ORR) experiments were conducted by performing linear sweep voltammetric (LSV) measurements on a rotating-disk electrode (RDE) in an O$_2$-saturated 0.1 M KOH electrolyte aqueous solution. Cyclic voltammetry (CV) and LSV curves were measured on a computer-controlled potentiostat (CHI 760C, CH Instrument, USA) with a three-electrode electrochemical cell. All the experiments were conducted at room temperature. Samples were casted on the GC working electrode, followed by casting with a Nafion solution (0.05 wt % in isopropanol) as the binder. A platinum wire was used as the counterelectrode, and a saturated calomel electrode (SCE) was used as the reference electrode.

2.2. Synthesis. 2.2.1. Preparation of GO-Cys. For the synthesis of the GO-Cys, 25 mg of dried GO was first suspended in distilled water (50 mL) by ultrasonication. The pH of GO dispersion was then adjusted to 10 by the addition of NaOH. Then 29 mg (0.024 mM) of Cys was added into the dispersion of GO. The mixture was heated to 80 °C and stirred constantly for 24 h. It could be observed that the color of the dispersion changed from dark brown to black without congregation during the reaction. After being cooled to room temperature, the resulting homogeneous black dispersion was subsequently filtered, washed, and redissolved in 20 mL of H$_2$O.

2.2.2. Preparation of Layer-by-Layer GO-Cys-GNR/ GNP Hybrid Nanostructure. *2.2.2.1. Preparation of GNP$_1$ (19.8 nm).* First, the water-soluble GNPs protected by surfactant were prepared based on the method described previously.[14] One hundred mL of 2.5 × 10^{-4} M HAuCl$_4$ aqueous solution was heated to 120 °C in an oil bath under vigorous stirring for 30 min. Then, 11 mL of 1% (wt %) sodium citrate aqueous solution was added into that solution with continued boiling. After 20 min, the purple−red solution was cooled to room temperature. Ten mL of the solution was centrifuged several times to remove excessive surfactants and other solution components and redispersed in water (10 mL). Thus, GNP$_1$ aqueous solution was prepared.

2.2.2.2. Preparation of GNP$_2$ (~49.7 nm). The water-soluble GNP$_2$ protected by surfactant were prepared based on the method described previously[14] with some modification. Into a flask was added 9 mL of the growth solution containing a mixture of 2.5 × 10^{-4} M HAuCl$_4$ and 0.01 M cetyl trimethylammonium bromide (CTAB). Warming was necessary to dissolve the CTAB. Fifty μL of 0.1 M freshly prepared ascorbic acid was added into the flask followed by gentle stirring for 2 min. Finally 0.5 mL of the above GNP$_1$ aqueous solution before centrifuge as Au seed was added into the flask,

and the mixture was kept at 30 °C in a water bath for at least 6 h. The solution was centrifuged several times to remove excessive surfactants and other solution components and redispersed in 15 mL of water. Thus, GNP$_2$ aqueous solution was prepared.

2.2.2.3. Preparation of GNR (~14.6 × 44.3 nm). The CTAB-coated GNRs were freshly prepared following the seed-mediated growth method[15] with some modification. For seed preparation specifically, 0.5 mL of an aqueous 0.01 M solution of HAuCl$_4$ was added to CTAB solution (15 mL, 0.1 M) in a vial. A bright brown−yellow color appeared. Then, 1.20 mL of 0.01 M ice-cold aqueous NaBH$_4$ solution was added all at once, followed by rapid inversion mixing for 2 min. The solution developed a pale brown−yellow color. Then, the vial was kept in a water bath maintained at 25 °C for future use. For nanorods growth, 9.5 mL of 0.1 M CTAB solution in water was added to a tube, and then 0.40 mL of 0.01 M HAuCl$_4$ and 0.06 mL of 0.01 M AgNO$_3$ aqueous solutions were added in this order and mixed by inversion. Then 0.06 mL of 0.1 M of ascorbic acid solution was added, and the resulting mixture at this stage becomes colorless. The seed solution (0.02 mL) was added to the above mixture tube, and the tube was slowly mixed for 10 s and left to sit still in the water bath at 25−30 °C for 3 h. The final solution turned purple within minutes after the tube was left undisturbed. The solution of CTAB-GNRs was centrifuged at 7500 rpm per 20 min several times to remove the excessive CTAB and other solution components and redispersed in 20 mL of water.

2.2.3. Preparation of Layer-by-Layer GO-Cys-GNP/ GNR Hybrid Nanostructure. For GO-Cys-GNP$_1$, first two 1.5 mL GO-Cys solutions were centrifuged at 14 000 rpm per 10 min twice to remove free cysteine. Second, after 15 min, 0.5 mL GNP$_1$ solution was added into it and the solution was mixed by magnetic stirring. Third, after 30 min, another centrifuged 1.5 mL of GO-Cys solution and 0.5 mL of GNP$_1$ solution were added one after another with a time interval of 15 min. Fourth, the previous step was repeated once more. Finally the mixture was sealed and stirred for 3 days. The GO-Cys-GNP$_2$ and GO-Cys-GNR were prepared by the same approach. The synthesis route of GO-Cys-GNR is presented in Figure 1. After reaction, the mixtures were centrifuged several times for purification.

3. RESULTS AND DISCUSSION

Figure 2 depicts a representative 3D layer-by-layer GO-Cys-GNR superstructure. When the primary amine reacts with GO, although multiple reactions might occur simultaneously, the major reaction under these conditions is an easy ring-opening reaction of the epoxy groups by the amine groups. A likely mechanism for this reaction involving nucleophilic attack at the α-carbon by the primary amine, leaving an open hydroxyl group, was demonstrated in the reaction of GO with octadecylamine.[16,17] Following the reaction yielding GO-Cys, as-prepared GNRs or GNPs are added to attach onto the GO-Cys layers via Au−S linkages. Here anisotropic GNRs (14.6 nm × 44.3 nm) were first used, and GNPs of different sizes (small GNP$_1$, ~19.8 nm; large GNP$_2$, ~49.7 nm) were further prepared to make a series of layer-by-layer nanostructures. The reported sizes are based on counting of 500 individuals for each type of NP. After this step, one observation clearly indicated the successful combination of GO and GNRs/GNPs: before addition of the GNRs/GNPs, the lightweight GO-Cys sheets could not fully precipitate during centrifugation, leaving a dark-
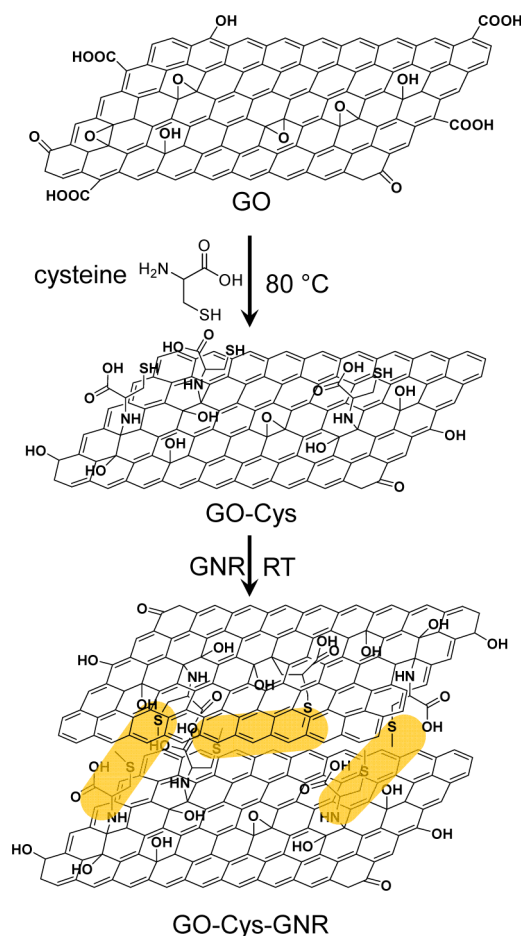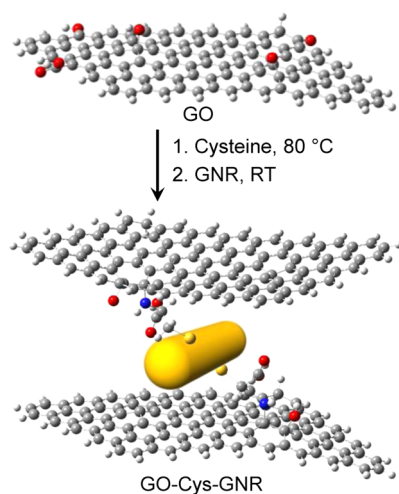
Figure 1. Synthesis of GO-Cys-GNR.

Figure 2. Scheme of the representative layer-by-layer graphene−GNR hybrid architecture. The structure shown is simplified, as there are multiple GNRs in the same layer and above and below there are continuously stacked GNRs and graphene layers.

black solution as the top layer; after addition of the GNRs/GNPs, the assembled hybrid structures were heavier, and most of the GO-Cys was pulled to the bottom during centrifugation, leaving a colorless top solution. The synthesis was also traced by UV−vis spectroscopy, as shown in Figure 3. Pristine GO showed a typical absorption peak at 230 nm. After reaction with Cys, this peak shifted to 253 nm, similar to observations for
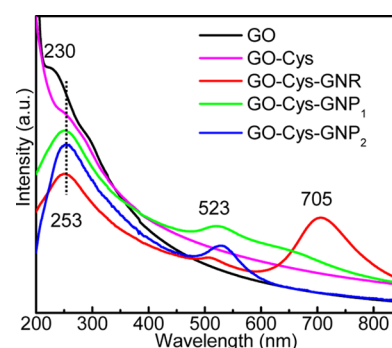

Figure 3. UV−vis spectra of GO, GO-Cys, GO-Cys-GNR, GO-Cys-GNP$_1$, and GO-Cys-GNP$_2$.

other reduction reactions.[18] After the subsequent combination with GNRs/GNPs, the typical localized surface plasmon resonance (LSPR) of GNPs/GNRs appeared. For anisotropic GNRs there are peaks at ca. 520 and 705 nm corresponding to the transverse and longitudinal LSPR, respectively. For spherical GNPs, there is a characteristic peak at ca. 520 nm.

The critical role of Cys in the successful binding of GNRs/GNPs and GO was confirmed by TEM (Figure 4). The GNR/
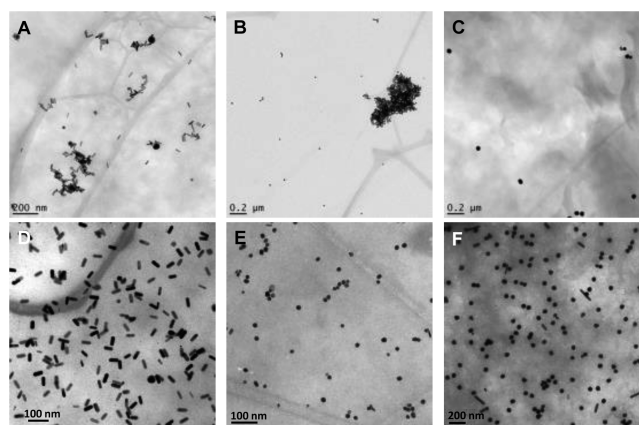

Figure 4. TEM images of (A−C) GO mixed with GNR, GNP$_1$, and GNP$_2$, respectively, and (D−F) GO-Cys-GNR, GO-Cys-GNP$_1$, and GO-Cys-GNP$_2$, respectively. The gray arcs and frames are from holey carbon films coated on TEM grids.

GNP solutions were simply mixed with GO-Cys solution to initiate the reaction. For comparison, samples were prepared by mixing GNR/GNP solutions with a solution of pristine GO under the same conditions. To prepare a TEM specimen, a droplet of each mixture was deposited on a holey, lacey, carbon-coated TEM grid. Suspended GO films were found on some of the holes. Figure 4A−C shows that, without the linking thiol group provided by Cys, the GNRs/GNPs tend to aggregate and very few of them are well-dispersed. In contrast, the GNRs/GNPs are attached to GO-Cys in a well-dispersed, uniform manner (Figure 4D−F). Although GNRs and GNPs tend to aggregate on the basis of electrostatic interactions,[15] when they were chemically bonded on the GO layers through Au−S linkages, the self-aggregation was prevented.

To illustrate the structural changes of GO after functionalization with Cys, the pristine GO and GO-Cys were analyzed by Raman spectroscopy, molecular simulation using Gaussian 09, X-ray photoelectron spectroscopy (XPS), and electron diffraction (ED). The typical Raman features of GO are
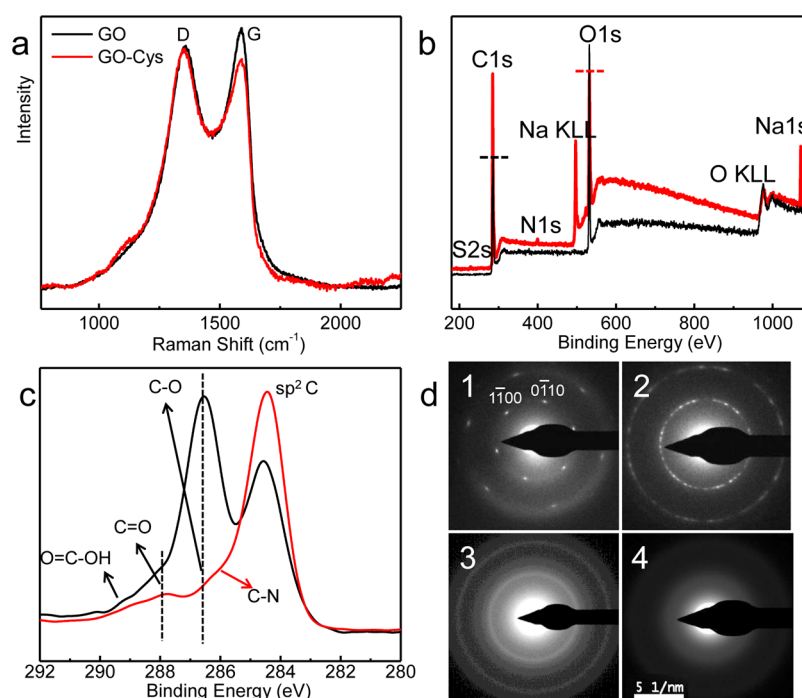
Figure 5. (a) Raman spectra of GO and GO-Cys. (b) XPS spectra and (c) high-resolution XPS spectra of GO and GO-Cys. The C−O peak of GO and the sp^2 C peak of GO-Cys have been normalized for easy comparison. (d) ED patterns of (1) single-layer GO, (2) multilayer GO, (3) GO-Cys, and (4) the carbon film substrate of the TEM grid.

displayed: one D band at 1353 cm^{-1} and one G band at 1592 cm^{-1} (see Figure 5a). The D band is due to the A_{1g} breathing vibrational mode of six-membered sp^2 carbon rings, which becomes Raman-active after neighboring sp^2 carbons are converted to sp^3 hybridization. The G band is due to the E_{2g} vibrational mode of sp^2-bonded carbon.[19] The intensity ratio of the D band to the G band (I_D/I_G) increases from 0.92 for GO to 1.04 for GO-Cys, indicating the formation of a higher number of surface defects. This could be ascribed to the chemical bonding of Cys and the reduction reaction at higher temperature. It has been discovered that, under this condition at 80 °C, the reduction reactions cause defunctionalization of epoxide, hydroxyl, and carboxylic acid groups.[20,21] The release of these oxygen-containing functional groups inevitably generates vacancies and topological defects on the reduced GO. Also, the relatively large Cys molecules attached on the GO surface further locally distort the flat structure compared with GO because of steric hindrance, resulting in some defects (see molecular simulation in Figure S1 of Supporting Information).

The chemical reaction of GO and Cys and the accompanying reduction reaction were confirmed by XPS measurements (Figure 5b, c). In Figure 5b, the existence of the N and S peaks at 398.8 and 228.8 eV, respectively, indicates the successful binding of Cys on GO. The significantly increased C 1s/O 1s ratio is due to the reduction of GO. The C content rose from 65 to 70%, and the O content dropped from 34 to 26%. The Na signal is due to the addition of NaOH for pH adjustment. For more detailed analysis, high-resolution C 1s spectra of GO and GO-Cys are shown in Figure 5c. The intensity of the C−O (286.2 eV), C═O (287.8 eV), and O═C−OH (289.2 eV) peaks all decreased significantly, indicating the release of O-rich groups. The new C−N component (a shoulder peak) at ∼286.1 eV in the C 1s spectrum of GO-Cys is attributed to the C−N bond between GO and Cys.

GO and GO-Cys were further studied by ED. The scattering patterns captured by TEM are shown in Figure 5d. The untreated single-layer and multilayer GO films exhibited distinct bright spots forming single and multiple sets of hexagons, indicating a relatively highly ordered graphene structure and a rather random stacking of GO sheets in multilayer films. Upon treatment with Cys, the bright spots were replaced by blurred ring patterns. The pronounced change in the ED pattern can be attributed to the stacking of a number of GO-Cys layers and an increase in defects in the GO-Cys sheets, which is consistent with the Raman and simulation results shown above.

The 3D layer-by-layer hybrid nanostructures were loaded on holey carbon film-coated TEM grids and then characterized. Because of their anisotropic shape, GNRs were easier to recognize and served as a good example for demonstration. The approach to illustrating the 3D nanostructure by tilting the sample is depicted in Figure 6a. TEM images are captured from the top view. Relative to GNR 0 in the middle layer as the reference, as the tilt angle θ is changed from negative to positive, GNR 1 in the middle layer, GNR 2 in the upper layer, and GNR 3 in the lower layer show different moves: 2 keeps moving toward 0; 1 first slightly moves away from 0 and then moves slightly toward 0; and 3 keeps moving away from 0. Because GNRs 1−3 all are to the left of GNR 0, their motion confirms that these GNRs are in different layers. The images of actual tilted samples are presented in Figure 6b, in which tilt angles of −40°, 0°, and 40° were chosen to display the significant shifts of GNRs. For each image, an enlarged area was picked for comparison. The chosen GNRs in different layers are marked with red, green, and blue circles and numbered according to Figure 6a. During tilting, the movements of GNRs 1−3 in different layers relative to GNR 0 were indeed different as described above. A video made as this sample was tilted with smooth continuous angle changes clearly proved the 3D
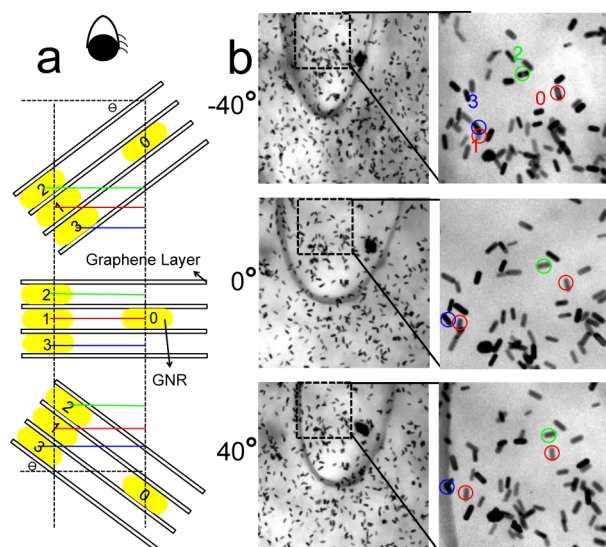
Figure 6. (a) Schematic depiction of the motion of GNRs in different layers during tilting as observed from the top. GNR 0 was used as the reference. The GNRs marked with different colors are in different layers. (b) TEM images of a 3D layer-by-layer GO-Cys-GNR sample at three different tilt angles. The gray arc in TEM images (b) is from holey carbon films coated on TEM grids.

structures (see the Supporting Information). In the images with continuous smaller tilting angle changes, the same results could be observed for GO-Cys-GNP$_1$ and GO-Cys-GNP$_2$ (Figure S2 and S3 of Supporting Information) as for GO-Cys-GNR.

On the basis of the TEM results for the tilted samples, side-view images of the 3D layer-by-layer nanostructures were generated by 3D tomography (TOMO) (Figures 7 and 8).
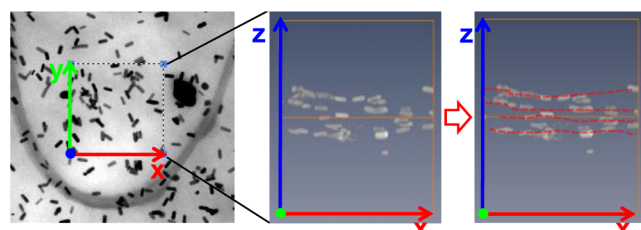

Figure 7. Side-view images of GO-Cys-GNR 3D nanostructures constructed by TOMO on the basis of TEM images. GNRs lying down in the same layer are connected by red dashed lines.

Figure 7 shows that, in a chosen small area, GNRs lie in different levels, and nearly all exhibit a lying down pattern because of their particular anisotropic shape. When GNRs at similar levels are connected by red dashed lines, layers appear. This indicates that the graphene sheets are in a parallel pattern rather than a random one in this 3D layer-by-layer nanostructure. This was further proved by SEM, as shown in Figure 9 and Figure S4 of the Supporting Information. In addition, with different GNR and GNP sizes (GNP$_1$ and GNP$_2$), the distance between graphene layers can be further tuned.

The electronic properties of the 3D hybrid architecture were investigated by oxidation reduction reaction (ORR) and cyclic voltammetry (CV) experiments.[2,22] The results are shown in Figure 10a along with those for GO and GO-Cys for comparison. The improvement in the ORR activity was confirmed by the increase in the onset potential and a
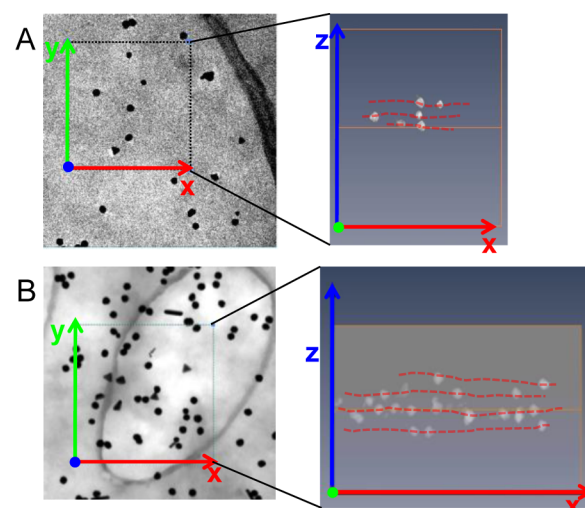

Figure 8. Side-view images of GO-Cys-GNP$_1$ and GO-Cys-GNP$_2$ 3D nanostructures constructed by TOMO based on TEM images.
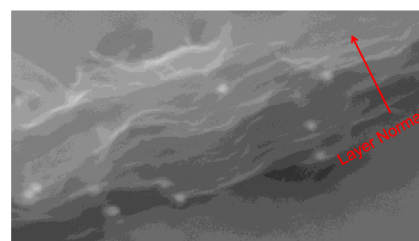

Figure 9. SEM image of the 3D layer-by-layer architecture from a GO-Cys-GNP$_2$ sample tilted by ca. 15°.

concomitant current density increase. After chemical modification, GO-Cys exhibited some improvement in ORR catalytic activity ($O_2 + 2H_2O + 4e^- \rightarrow 4OH^-$). When it was further combined with GNPs or GNRs, much higher catalytic activities were observed. The onset potential for GO was about −0.30 V, compared with GO-Cys (−0.28 V), GO-Cys-GNP$_1$ (−0.23 V), GO-Cys-GNP$_2$ (−0.24 V), and GO-Cys-GNR (−0.22 V). When GNPs and GNRs were incorporated into the system, the metal nanoparticles increased the ORR activity significantly. In the CV experiments (Figure 10b), from GO to GO-Cys there was not an obvious peak shift. After the addition of GNPs/GNRs, the peak shifted to less negative positions, indicating that the materials were easier to reduce. Also, the current density significantly jumped from the reduction scans to the oxidation scans. Particularly for GO-Cys-GNP$_1$, the cyclic voltammogram displayed a shape close to rectangular, which means that this material has good potential for applications such as supercapacitors.[22] In an ideal situation, it can be envisioned that the entire surface of graphene within such 3D layer-by-layer hybrid nanomaterials would be exposed to electrolyte ions to facilitate the charging/recharging process of the devices through the large interstitial space.

4. CONCLUSIONS

In conclusion, a facile solution-processable strategy for creating a 3D layer-by-layer nanostructure by sandwiching GNPs between graphene layers was for the first time developed. Cys, which contains amino and thiol groups, was reacted with GO via the amine group and then further linked to GNRs via formation of covalent Au−S linkages. The GNRs were found to
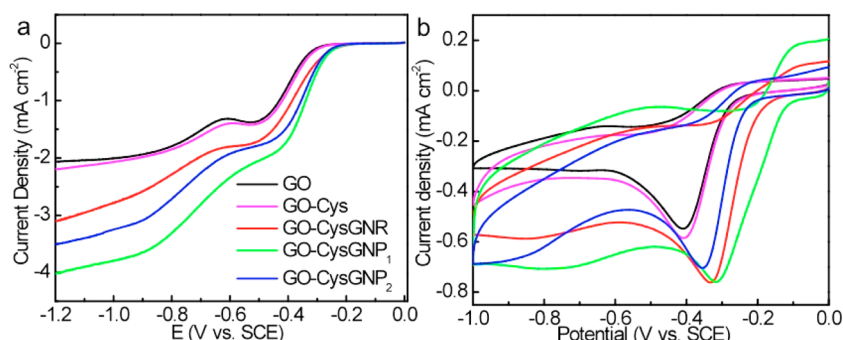
Figure 10. (a) Linear sweep voltammetric (LSV) curves for oxygen reduction at the GO, GO-Cys, GO-Cys-GNP$_1$, GO-Cys-GNP$_2$, and GO-Cys-GNR in an O$_2$-saturated 0.1 M KOH solution at a scan rate of 10 mVs^{-1}. The electrode rotation speed was 1600 rpm. (b) CV experiment of GO, GO-Cys, GO-Cys-GNP$_1$, GO-Cys-GNP$_2$, and GO-Cys-GNR.

separate the graphene sheets well within the 3D layer-by-layer structure. GO before and after the reaction with Cys was investigated by UV−vis, Raman, XPS, and ED analyses, which indicated not only that Cys molecules were attached on GO but also that GO endured a reduction reaction. The 3D layer-by-layer architectures were confirmed using TEM and SEM by tilting the samples. Furthermore, when GNPs with different sizes were introduced, the distance between graphene layers could be controlled, offering an opportunity to investigate the effect of the interlayer distance on properties of the 3D graphene materials.[23] ORR and CV measurements indicated that these 3D hybrid nanomaterials possess good electrochemical activities, which have potential in applications such as fuel cells and supercapacitors. This work provides an exciting impetus for building a tunable 3D carbon nanostructure with tailored functionality. In future work, CNTs are expected to be sandwiched between graphene layers in this 3D hybrid nanostructure, allowing coherent 3D carbon nanostructures to be built.

■ ASSOCIATED CONTENT

Ⓢ Supporting Information

Molecular simulations, tilted samples of GO-Cys-GNR, GO-Cys-GNP$_1$, and GO-Cys-GNP$_2$, and a video of tilted GO-Cys-GNR sample in TEM. This material is available free of charge via the Internet at http://pubs.acs.org.

■ AUTHOR INFORMATION

Corresponding Author

*E-mail: qli1@kent.edu.

Notes

The authors declare no competing financial interest.

■ ACKNOWLEDGMENTS

■ REFERENCES

(1) Novoselov, K. S.; Geim, A. K.; Morozov, S. V.; Jiang, D.; Zhang, Y.; Dubonos, S. V.; Grigorieva, I. V.; Firsov, A. A. Electric field effect in atomically thin carbon films. *Science* **2004**, *306*, 666−669.

(2) Gong, K. P.; Du, F.; Xia, Z. H.; Dustock, M.; Dai, L. M. Nitrogen-doped carbon nanotube arrays with high electrocatalytic activity for oxygen reduction. *Science* **2009**, *323*, 760−764.

(3) Li, X. S.; Cai, W. W.; An, J. H.; Kim, S.; Nah, J.; Yang, D. X.; Piner, R.; Velamakanni, A.; Jung, I.; Tutuc, E.; Banerjee, S. K.; Colombo, L.; Ruoff, R. S. Large-area synthesis of high-quality and uniform graphene films on copper foils. *Science* **2009**, *324*, 1312−1314.

(4) Sun, Y.; Wu, Q.; Shi, G. Graphene based new energy materials. *Energy Environ. Sci.* **2011**, *4*, 1113−1132.

(5) Frackowiaka, E.; Beguin, F. Electrochemical storage of energy in carbon nanotubes and nanostructured carbons. *Carbon* **2002**, *40*, 1775−1787.

(6) Varshney, V.; Patnaik, S. S.; Roy, A. K.; Froudakis, G.; Farmer, B. L. Modeling of thermal transport in pillared-graphene architectures. *ACS Nano* **2010**, *4*, 1153−1161.

(7) Dimitrakakis, G. K.; Tylianakis, E.; Froudakis, G. E. Pillared graphene: A new 3-D network nanostructure for enhanced hydrogen storage. *Nano Lett.* **2008**, *8*, 3166−3170.

(8) Mao, Y. L.; Zhong, J. X. The computational design of junctions by carbon nanotube insertion into a graphene matrix. *New J. Phys.* **2009**, *11*, 093002.

(9) Du, F.; Yu, D. S.; Dai, L. M.; Ganguli, S.; Varshney, V.; Roy, A. K. Preparation of tunable 3D pillared carbon nanotube−graphene networks for high-performance capacitance. *Chem. Mater.* **2011**, *23*, 4810−4816.

(10) Dai, L. M. Functionalization of graphene for efficient energy conversion and storage. *Acc. Chem. Res.* **2013**, *46*, 31−42.

(11) Si, Y. C.; Samulski, E. T. Exfoliated graphene separated by platinum nanoparticles. *Chem. Mater.* **2008**, *20*, 6792−6797.

(12) Yin, P. T.; Kim, T.-H.; Choic, J.-W.; Lee, K.-B. Prospects for graphene−nanoparticle-based hybrid sensors. *Phys. Chem. Chem. Phys.* **2013**, *15*, 12785−12799.

(13) Han, S.-T.; Zhou, Y.; Wang, C. D.; He, L. F.; Zhang, W. J.; Roy, V. A. L. Layer-by-layer-assembled reduced graphene oxide/gold nanoparticle hybrid double-floating-gate structure for low-voltage flexible flash memory. *Adv. Mater.* **2013**, *25*, 872−877.

(14) Huang, Y. J.; Kim, D. H. Synthesis and self-assembly of highly monodispersed quasispherical gold nanoparticles. *Langmuir* **2011**, *27*, 13861−13867.

(15) Murphy, C. J.; San, T. K.; Gole, A. M.; Orendorff, C. J.; Gao, J. X.; Gou, L.; Hunyadi, S. E.; Li, T. Anisotropic metal nanoparticles: Synthesis, assembly, and optical applications. *J. Phys. Chem. B* **2005**, *109*, 13857−13870.

(16) Wang, S.; Chia, P.-J.; Chua, L.-L.; Zhao, L.-H.; Png, R.-Q.; Sivaramakrishnan, S.; Zhou, M.; Goh, R. G.-S.; Friend, R. H.; Wee, A. T.-S.; Ho, P. K.-H. Band-like transport in surface-functionalized highly solution-processable graphene nanosheets. *Adv. Mater.* **2008**, *20*, 3440−3446.

(17) Yang, H. F.; Shan, C. S.; Li, F. H.; Han, D. X.; Zhang, Q. X.; Niu, L. Covalent functionalization of polydisperse chemically-converted graphene sheets with amine-terminated ionic liquid. *Chem. Commun.* **2009**, 3880−3882.

(18) Liu, J. B.; Li, Y. L.; Li, Y. M.; Li, J. H.; Deng, Z. X. Noncovalent DNA decorations of graphene oxide and reduced graphene oxide toward water-soluble metal−carbon hybrid nanostructures via self-assembly. *J. Mater. Chem.* **2010**, *20*, 900−906.

(19) Zhou, Y.; Bao, Q.; Tang, L. A. L.; Zhong, Y.; Loh, K. P. Hydrothermal dehydration for the "green" reduction of exfoliated graphene oxide to graphene and demonstration of tunable optical limiting properties. *Chem. Mater.* **2009**, *21*, 2950−2956.

(20) Cui, P.; Seo, S.; Lee, J.; Wang, L.; Lee, E.; Min, M.; Lee, H. Nonvolatile memory device using gold nanoparticles covalently bound to reduced graphene oxide. *ACS Nano* **2011**, *5*, 6826−6833.

(21) Dai, B. Y.; Fu, L.; Liao, L.; Liu, N.; Yan, K.; Chen, Y. S.; Liu, Z. F. High-quality single-layer graphene via reparative reduction of graphene oxide. *Nano Res.* **2011**, *4*, 434−439.

(22) You, B.; Li, N.; Zhu, H. Y.; Zhu, X. L.; Yang, J. Graphene oxide-dispersed pristine cnts support for MnO_2 nanorods as high performance supercapacitor electrodes. *ChemSusChem* **2013**, *6*, 474−480.

(23) de Andres, P. L.; Ramírez, R.; Vergés, J. A. Strong covalent bonding between two graphene layers. *Phys. Rev. B* **2008**, *77*, 045403.

15338

dx.doi.org/10.1021/jp504553w | *J. Phys. Chem. C* 2014, 118, 15332−15338